⌘ *Author's Choice*

THE JOURNAL OF BIOLOGICAL CHEMISTRY VOL. 286, NO. 40, pp. 34839–34850, October 7, 2011
© 2011 by The American Society for Biochemistry and Molecular Biology, Inc. Printed in the U.S.A.

Importance of Shank3 Protein in Regulating Metabotropic Glutamate Receptor 5 (mGluR5) Expression and Signaling at Synapses*[S]

Received for publication, May 6, 2011, and in revised form, July 18, 2011 Published, JBC Papers in Press, July 27, 2011, DOI 10.1074/jbc.M111.258384

Chiara Verpelli[‡§1], Elena Dvoretskova[¶1], Cinzia Vicidomini[‡], Francesca Rossi[‡], Michela Chiappalone[¶], Michael Schoen[‖], Bruno Di Stefano[**], Renato Mantegazza[§], Vania Broccoli[**], Tobias M. Böckers[‖], Alexander Dityatev[¶2], and Carlo Sala[‡§3]

*From the [‡]Department of Pharmacology, CNR Institute of Neuroscience, University of Milan, Milan 20129, the [§]Department of Neuromuscular Diseases and Neuroimmunology, Neurological Institute Foundation Carlo Besta, Milan 20133, the [¶]Department of Neuroscience and Brain Technologies, Istituto Italiano di Tecnologia, Genova 16163, [‖]Institute of Anatomy and Cell Biology, Ulm University Faculty of Medicine, Ulm 89081, and the **Division of Neuroscience, San Raffaele Scientific Institute, Milan 20132, Italy*

Shank3/PROSAP2 gene mutations are associated with cognitive impairment ranging from mental retardation to autism. Shank3 is a large scaffold postsynaptic density protein implicated in dendritic spines and synapse formation; however, its specific functions have not been clearly demonstrated. We have used RNAi to knockdown Shank3 expression in neuronal cultures and showed that this treatment specifically reduced the synaptic expression of the metabotropic glutamate receptor 5 (mGluR5), but did not affect the expression of other major synaptic proteins. The functional consequence of Shank3 RNAi knockdown was impaired signaling via mGluR5, as shown by reduction in ERK1/2 and CREB phosphorylation induced by stimulation with (*S*)-3,5-dihydroxyphenylglycine (DHPG) as the agonist of mGluR5 receptors, impaired mGluR5-dependent synaptic plasticity (DHPG-induced long-term depression), and impaired mGluR5-dependent modulation of neural network activity. We also found morphological abnormalities in the structure of synapses (spine number, width, and length) and impaired glutamatergic synaptic transmission, as shown by reduction in the frequency of miniature excitatory postsynaptic currents (mEPSC). Notably, pharmacological augmentation of mGluR5 activity using 3-cyano-*N*-(1,3-diphenyl-1*H*-pyrazol-5-yl)-benzamide as the positive allosteric modulator of these receptors restored mGluR5-dependent signaling (DHPG-induced phosphorylation of ERK1/2) and normalized the frequency of mEPSCs in Shank3-knocked down neurons. These data demonstrate that a deficit in mGluR5-mediated intracellular signaling in Shank3 knockdown neurons can be compensated by 3-cyano-*N*-(1,3-diphenyl-1*H*-pyrazol-5-yl)-benzamide; this raises the possibility that pharmacological augmentation of mGluR5 activity represents a possible new therapeutic approach for patients with Shank3 mutations.

Haploinsufficiency of the *SHANK3*/*PROSAP2* gene, which encodes a structural protein located in the postsynaptic density (PSD)[4] and involved in spine maintenance in hippocampal neurons (1), is likely to be an essential cause of the major neurological features associated with the 22q13 deletion/Phelan-McDermid syndrome. Disruption of *SHANK3*/*PROSAP2* was first reported by Bonaglia *et al.* (2). Its association with the neurological deficit related to the syndrome is strongly supported by the observation that all 22q13 deletions analyzed, except one (3), concerned *SHANK3* (4), as shown by both the identification of a recurrent breakpoint within the *SHANK3* gene (5) and by the recent finding that *SHANK3* mutations can result in language and/or social interaction impairment (6). More recently, other small interstitial deletions or missense mutations in *SHANK3* have been strongly associated with autism spectrum disorder and mental retardation (7–9).

The three genes, *SHANK1, SHANK2,* and *SHANK3,* encode large scaffold proteins that contain an ankyrin repeat near the N terminus followed by an Src homology domain 3 domain, a PDZ domain, a long proline-rich region, and a sterile α motif domain at the C terminus (10). These proteins molecularly link the two glutamate receptor subtypes, NMDA receptors and type-I metabotropic GluRs (mGluRs). The Shank PDZ domain binds to the C terminus of GKAP, which binds to the PSD-95·NMDA receptor complex. Homer interaction with the proline-rich domain ensures the association of Shank with type I mGluRs (mGluR1 and mGluR5) (11–13).

Overexpression of Shank1 in rat hippocampal neurons accelerates the maturation of filopodia-like protrusions in mature spines and promotes the enlargement of mature spines (14–

* This work was supported in part by Telethon-Italy Grant GGP09196, Fondazione CARIPLO Project number 2009.264, RSTL-CNR, Regione Lombardia Project number SAL-50-16983 TERDISMENTAL, and an Italian Institute of Technology, Seed Grant (to C. S. and V. B.).

⌘ *Author's Choice*—Final version full access.

[S] The on-line version of this article (available at http://www.jbc.org) contains supplemental Fig. S1.

[1] Both authors contributed equally to this work.

[2] Supported by a grant from the San Paolo Foundation and the Italian Institute of Technology.

[3] To whom correspondence should be addressed: Via Vanvitelli 32, 20129 Milano, Italy. Tel.: 39-02-50317096; Fax: 39-02-7490574; E-mail: c.sala@in.cnr.it.

[4] The abbreviations used are: PSD, postsynaptic density; mGluR, metabotropic glutamate receptor; DHPG, (*S*)-3,5-dihydroxyphenylglycine; CREB, cAMP-response element-binding protein; CDPPB, 3-cyano-*N*-(1,3-diphenyl-1*H*-pyrazol-5-yl)-benzamide; DIV, days *in vitro*; TTX, tetrodotoxin; APV, 2-amino-5-phosphonopentanoic acid; mEPSC, miniature excitatory postsynaptic current; HBS, HEPES-buffered saline; ANOVA, analysis of variance; LTD, long-term depression.

16). In contrast, mice lacking Shank1 display smaller dendritic spines, weaker synaptic transmission, and altered spatial learning (17). Shank3 overexpression in rat cerebellar granule cells induces dendritic spine and synapse formation, whereas Shank3 knockdown in hippocampal neurons reduces the number of dendritic spines (1). Both Shank1 and Shank3 may form structural frameworks in the PSD via different molecular mechanisms (18, 19).

Several splice variants have been described for all three genes, in particular six intragenic promoters generating multiple splicing variants have been identified for *SHANK3* (20, 21). The functional role for all these splice variants remains to be determined; however, one can postulate that, depending on the introduced mutations, the resulting truncated proteins might have different functional consequences, such as gain or loss of specific functions.

This might explain the contradictory results recently published on Shank3 partial-KO mice. Wang *et al.* (21) and Bozdagi *et al.* (54) showed an alteration in hyppocampal synapse properties, whereas Peca *et al.* (22) found clear alterations only in the cortico-striatal synapses. Finally Bangash *et al.* (23) described a gain-of-function phenotype for Shank3 protein missing the C-terminal fragment, which reduce specifically NR1 at synapses. With the aim of understanding the function of Shank3 and its isoform(s) in the overall neuronal network toward the identification of therapeutic target(s), for patients affected with MR and autism due to SHANK3 mutations, we have studied the synaptic molecular pathways in cultured murine Shank3 knockdown neurons.

Rather than using Shank partial knockout mice, we knocked down the expression of all the major Shank3 splice variants in neuronal cultures through RNA interference (RNAi). Our data show that knockdown of Shank3 expression in rat and/or mouse hippocampal cell cultures induces a specific reduction in expression of mGluR5 receptors, as well as a reduction in (*S*)-3,5-dihydroxyphenylglycine (DHPG) (a group I mGluR agonist)-induced ERK1/2 and CREB phosphorylation and in mGluR5-dependent synaptic plasticity and modulation of neural network activity. Notably, pharmacological augmentation of mGluR5 activity using 3-cyano-*N*-(1,3-diphenyl-1*H*-pyrazol-5-yl)-benzamide (CDPPB) as a positive allosteric modulator potentiated mGluR5-dependent signaling (DHPG-induced phosphorylation of ERK1/2) and restored synaptic physiology in neurons knocked down for Shank3. Thus, unlike Shank1, which in association with Homer acts as a structural framework at synapses (19), Shank3 could act as a signaling scaffold platform at synapses.

EXPERIMENTAL PROCEDURES

Neuronal Cultures—Rat hippocampal or cortical neuronal cultures were prepared from 18- to 19-day-old rat embryos (pregnant female rats were obtained from Charles River Laboratories). Neurons were plated at high density (750–1000 cells/mm^2) and medium density (150–200 cells/mm^2) and grown as described (24) using B27 prepared in the laboratory. Neurons were plated onto 6-well plastic tissue culture plates (Iwaki, Bibby Sterilin), or 18-mm diameter coverslips and grown on 12-well plastic tissue culture plates (Iwaki, Bibby Sterilin). Primary mouse hippocampal neuronal cultures were prepared as described previously (25). Hippocampi from 1- to 3-day-old C57BL6/J mouse pups were dissected at 4 °C, and plated at a density of 300/mm^2 in Neurobasal-A medium supplemented with 2% B27 supplement and 25 μg/ml of FGF2 (both from Invitrogen) on 18-mm diameter round glass coverslips (Menzel-Glaser) coated overnight with 100 μg/ml of poly-L-lysine and 40 μg/ml of laminin (both from Sigma). From culture day 3, the medium was supplemented with 0.5 μM AraC (Sigma) to prevent glial cell proliferation. Neurons were transfected using calcium phosphate precipitation as per the protocol described by Sala *et al.* (14). Cultures were infected with lentivirus expressing shRNA specific for luciferase (shCtrl) or Shank3 (shShank3) on day 7 *in vitro* (DIV) and used for experiments on 13–15 DIV. Cells were stimulated with 100 μM DHPG, 100 μM NMDA, or 50 mM KCl at 15 DIV for 30 min. To reduce endogenous synaptic activity, 2 μM tetrodotoxin (TTX) was added to cultures 12 h before stimulation. For the biochemical experiments with CDPPB (Calbiochem), neurons were treated for 12 h with 100 nM or 1 μM CDPPB before DHPG stimulation.

RNA Interference and Relevant Plasmids—For plasmid-based RNA inhibition, Shank3 and luciferase (26) oligonucleotides were annealed and inserted into the HindIII/BglII sites of the pLVTHM vector for lentivirus production of the shRNA. We used the following siRNA sequence that targets exon 21 of the rat and mouse *SHANK3* gene (GenBank^{TM} accession number NM_021676 and NM_021423.3): 5′-GGAAGTCACCAGAGGACAAGA-3′. The Shank3 rescue (Shank3r), R87C (Shank3R87Cr), and InsG (Shank3InsGr) constructs resistant to interference by siRNA were generated by changing six nucleotides of the siRNA target site, without changing the amino acid sequence of the resultant protein. Shank3 R87C and InsG mutants have been described elsewhere (6).

Real Time-PCR (RT-PCR)—Total mRNA was extracted using the RNeasy Plus kit (Qiagen, Valencia, CA). cDNA was synthesized from DNase I-treated RNA using the QuantiTect reverse transcription kit (Qiagen,) according to the manufacturer's instructions. mRNA transcripts were quantified by TaqMan Q-PCR 3 (Applied Biosystems) on a Prism 7900 thermal cycler and sequence detector (Applied Biosystems). All primers and probes were from Applied Biosystems. Reactions were performed in triplicate. Average Δ-C_t values normalized to GAPDH or cyclophilin A (housekeeping genes) were used to calculate gene-fold induction in treated samples, relative to control set to 1.

Antibodies—The following antibodies were used: rabbit anti-Shank3 (Santa Cruz Biotechnology, H-160); guinea pig anti-Shank3 (27); rabbit anti-ERK1/2, rabbit anti-pERK 1/2, rabbit anti-eEF2, and rabbit anti-GFP 1:500 (Cell Signaling Technology); rabbit anti-mGluR1, rabbit anti-mGluR5, rabbit anti-mGluR4, rabbit anti-GluR1, and rabbit anti-GluR2/3 (Millipore Bioscience Research Reagents); mouse anti-GluR2, mouse anti-NR2B, mouse anti-Shank1, mouse anti-Shank2, mouse anti-Pan Shank, and mouse anti-PSD95 (NeuroMab, University of California, Davis/NIH NeuroMab Facility); rabbit anti-GKAP (gifts from Morgan Sheng, Genentech); rabbit anti-Homer (gifts from Eunjoon Kim, KAIST, South Corea); rabbit anti-IRSp53 and mouse anti-Abi1 (gifts from Giorgio Scita, IFOM-

IEO, Italy); mouse anti-synaptophysin, mouse anti-β-actin, and mouse anti-α-tubulin (Sigma); secondary FITC-, Cy3- and Cy5-conjugated anti-mouse, anti-rabbit, anti-guinea pig, or anti-goat antibodies (Jackson ImmunoResearch); secondary HRP-conjugated anti-mouse, anti-rabbit, anti-guinea pig, or anti-goat (GE Healthcare).

Western Blotting—Western blotting was performed as described in Ref. 28. The signal was detected using an ECL detection system (PerkinElmer Life Sciences). The intensity of the bands was measured with ImageJ software. Signals of the detected proteins were normalized according to signals for actin or tubulin; the intensity of phosphospecific ERK1/2 and CREB immunoreactivity was normalized to the total ERK1/2 and CREB signal in the same lane. Changes in protein levels and in ERK1/2 and CREB phosphorylation were compared with those of untreated samples and were expressed as fold-increase or decrease. The results are shown as mean ± S.E.

Immunocytochemistry—Neurons were fixed in 4% paraformaldehyde and 4% sucrose at room temperature or in 100% methanol at −20 °C. Primary and secondary antibodies were applied in GDB buffer (30 mM phosphate buffer, pH 7.4, containing 0.2% gelatin, 0.5% Triton X-100, and 0.8 M NaCl) for 2 h at room temperature or overnight at 4 °C.

To study ERK1/2 phosphorylation, neurons were transfected with the pEGFP, Shank3r, Shank3R87Cr, or Shank3InsGr vectors alone or in combination with Shank3 shRNA at a ratio of 1:2. Confocal images were acquired as described below. Cell bodies were manually traced using MetaMorph software (Molecular Devices) on the GFP channel. The average intensity of the fluorescent signal obtained with antibody against pERK1/2 in the transfected neurons was divided by the average intensity of the pERK1/2 signal in adjacent untransfected neurons.

To estimate cell surface expression of the GluR1 subunit of AMPA receptors and its down-regulation by DHPG (29), untreated or DHPG-treated cultures were briefly washed with PBS and incubated with antibody against an extracellular epitope of the GluR1 subunit (Alomone Labs, agc-004, 16 μg/ml) for 15 min at 37 °C. For treatment, either 100 μM DHPG + 50 μM 2-amino-5-phosphonopentanoic acid (APV) or 50 μM APV alone were added to the culture medium for 10 min at 37 °C. Following incubation with anti-GluR1 antibody, cultures were fixed with 4% formaldehyde. Anti-rabbit Alexa 546-conjugated antibody (Invitrogen) was applied under nonpermeabilizing conditions for 1 h at RT.

All images were collected using a Leica TCS SP5 confocal microscope and ×60 oil immersion objective at 1024 × 1024 pixel resolution. The quantitative analysis was performed using a Z-series projection of five images taken at 0.8-μm depth intervals. All analyses were performed using NIH ImageJ software. The threshold for detection of GluR1-positive fluorescent clusters was fixed at twice the level of background fluorescence obtained from a region of diffuse fluorescence within the dendritic shaft. Only clusters lying along secondary dendritic branches were counted; regions in which the identification of neuronal processes was ambiguous were excluded from the quantification. We quantified the number of GluR1 immunoreactive clusters per 100-μm dendritic length within a given field.

Measurement of Dendritic Spine Morphology—Neurons were cotransfected with a shRNA vectors and DsRed at a ratio of 2:1 (7.5 μg of total DNA/well in 12-well plates) on 7 DIV and fixed on 18 DIV. Labeled transfected neurons were randomly chosen for quantification in at least four independent experiments for each construct.

Confocal images of 1024 × 1024 pixels were obtained with a LSM 510 Meta confocal microscope (Carl Zeiss, a gift from Fondazione Monzino) and a ×63 objective with sequential acquisition settings. Each image was a Z-series projection of 7–15 images, each averaged two to four times, and taken at 0.4–0.7-μm depth intervals. Morphometric measurements were made using MetaMorph software (Molecular Devices). Individual dendrites were selected randomly and their spines were traced manually. The maximum length and head width of each spine were measured and archived automatically (30).

Electrophysiology—Cells were used for electrophysiological recordings 3–4 days after transfection. For rescue experiments, the infected neurons were transfected on 11 DIV with pcDNA3 (Mock) or Shank3 resistant to shShank3 (Shank3r) cloned in pcDNA3. A vector expressing a red fluorescent protein tdTomato (31) was co-transfected in these experiments to allow the identification of transfected neurons.

For pharmacological rescue of frequency of mEPSCs, the allosteric modulator of mGluR5 (CDPPB, 1 μM, dissolved in 0.1% dimethyl sulfoxide) was applied overnight on 13 DIV and during recordings of mEPSCs on 14 DIV. As a vehicle control, 0.1% dimethyl sulfoxide was used.

Whole cell recordings from pyramidal-like neurons were obtained as previously described (29). Electrodes with a resistance in the range of 3–6 megohms were filled with a solution that contained 130 mM $CsMeSO_4$, 8 mM NaCl, 4 mM MgATP, 0.3 mM NaGTP, 0.5 mM EGTA, and 10 mM HEPES, pH 7.25. Cells were perfused continuously with HEPES-buffered saline (HBS) of the following composition: 119 mM NaCl, 5 mM KCl, 2 mM $CaCl_2$, 2 mM $MgCl_2$, 25 mM HEPES, 33 mM D-glucose, 0.5 μM TTX citrate (Tocris), and 0.05 mM picrotoxin (Tocris), pH 7.35. The osmolarity of HBS was adjusted to that of the culture medium on the day of recording. The osmolarity of the electrode solution was 10 mosmol less than that of HBS. When used, DHPG (100 μM, Tocris) was added to HBS. To prevent any contribution of NMDA receptor-dependent long-term depression (LTD) and thus elicit pure mGluR-dependent LTD, 50 μM APV (Sigma) was co-applied with DHPG or applied alone as a control. Data were digitized at 10 kHz. Continuous recording of mEPSCs was made using an EPC10 USB patch clamp amplifier and PATCHMASTER software (HEKA Elektronik). Detection and measurements of mEPSCs, which were collected over a 3-min period, were performed using MiniAnalysis software (Synaptosoft, Leonia, NJ) after filtering traces at 1 kHz and using a detection threshold of 6 pA (*i.e.* above 4 times the standard deviation of baseline noise) and visual verification of all detected events. Only cells with a holding current less than −100 pA were analyzed.

Microelectrode Array (MEA) Recordings and Analysis—Microelectrode arrays (Multichannel Systems, MCS, Reutlingen,

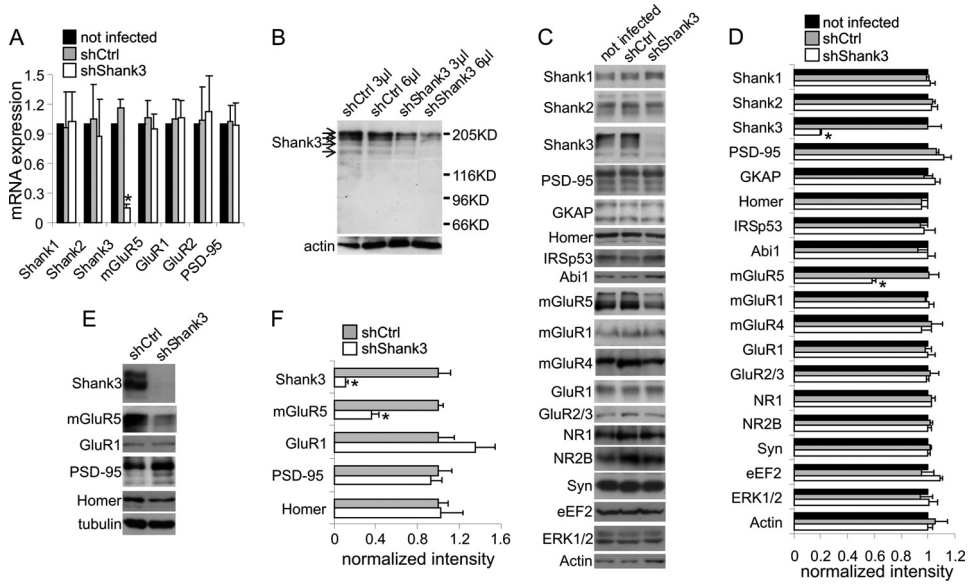

FIGURE 1. **Knocking down Shank3 reduces mGluR5 expression.** *A*, histogram showing mean ± S.E. for four independent experiments, of mRNA levels of the indicated proteins (normalized against those of uninfected neurons) in hippocampal neurons infected or not with a lentivirus expressing shShank3 or control shRNA (*shCtrl*); the level of Shank3 mRNA was significantly lower in the shShank3-infected neurons than in uninfected or shCtrl-infected neurons, *, $p < 0.01$, Student's *t* test. *B*, Western blot of hippocampal neurons infected with 3 and 6 μl of lentivirus preparations expressing shShank3 or shCtrl and Shank3; Shank3 was detected using rabbit H-160 anti-Shank3 antibody. The four major bands recognized by the antibody are indicated by the *arrows*. *C*, Western blot of hippocampal neurons infected at 7 DIV with a lentivirus expressing shShank3 or shCtrl, as indicated *above* the panels, and analyzed with the antibodies against the proteins indicated on the *left side* of the panels. *D*, histogram showing mean ± S.E. for four independent experiments, of protein levels (normalized against those of the uninfected neurons) in the hippocampal neurons infected with a lentivirus expressing shShank3 or shCtrl. The expression levels of Shank3 and mGluR5 were significantly lower in the shShank3-infected neurons than in uninfected and shCtrl-infected neurons; *, $p < 0.01$, Student's *t* test. *E*, Western blot of synaptosomes obtained from hippocampal neurons infected with a lentivirus expressing shShank3 or shCtrl and analyzed with the antibodies against the proteins indicated on the *left side* of the panel. *F*, histogram showing mean ± S.E. for three independent experiments, of protein levels (normalized against those of the shCtrl infected neurons) in synaptosomes obtained from hippocampal neurons infected with a lentivirus expressing shShank3 or shCtrl. The expression levels of Shank3 and mGluR5 were significantly lower in the shShank3-infected neurons than in uninfected and shCtrl-infected neurons; *, $p < 0.01$, Student's *t* test.

Germany) consisted of 60 TiN/SiN planar round electrodes (30 μm diameter, 200-μm center to center interelectrode distance) arranged in an 8 × 8 square grid excluding corners. Dissociated neurons from C57BL6/J mice at postnatal day 1 were infected on 8–10 DIV as described above. The activity of all cultures was recorded using the MEA60 System (MCS). After ×1200 amplification, signals were sampled at 10 kHz and acquired through the data acquisition card and MC_Rack software (MCS). To reduce thermal stress to the cells during the experiment, MEAs were kept at 37 °C by means of a controlled thermostat (MCS) and covered by flexible polydimethylsiloxane lids (32), to avoid evaporation and prevent changes in osmolarity. There was one recording session per culture; the session included 30 min of baseline recordings in the absence of DHPG and three consecutive 30-min recordings in the presence of 1, 10, and 100 μM DHPG. Only the last 20 min of each episode were analyzed to exclude the initial part of recordings, during which neuronal activity may have been influenced by the mechanical disturbances evoked by injection of the drug. Only cultures in which more than 70% Shank3 expression was knocked out were included in the analysis.

Data analysis was performed off-line using custom software, SPYCODE, developed in MATLAB® (The Mathworks) (33); this software collects a series of tools for processing of multichannel neural recordings. Data were imported into MATLAB from mcd files (MCS format), and spikes were detected using the precise timing spike detection algorithm (34). Spike trains were analyzed using a custom burst detection method (35), the parameters of which are directly estimated from the inter-spike interval distribution of each channel. Following the burst detection procedure, several measures describing spike and burst statistics were extracted; these included mean firing rate, mean bursting rate, mean burst duration, mean frequency intra burst (spikes/sec), and percentage and frequency of out-burst spikes (*i.e.* spikes not included in bursts over the total). Two-way ANOVA with repeated measures followed by Holm-Sidak pairwise comparison of groups was used for statistical evaluation of the DHPG and shShank3 effects.

RESULTS

To understand the role of Shank3 in synapse formation and function, we knocked down Shank3 using RNA interference. Expressed via a lentiviral vector, Shank3 shRNA (shShank3) strongly reduced the levels of endogenous Shank3 mRNA and protein, but not those of other Shank family members, in murine hippocampal cultures; a control shRNA (shCtrl) had no such effect (Fig. 1, *A*, *C*, and *D*). Interestingly, Shank3 shRNA knocked down all four major Shank3 isoforms in a dose-dependent manner (Fig. 1*B*). We used two different antibodies in our immunoblotting analysis, one against the N-terminal domain and one against the C-terminal domain (see supplemental Fig. 1*A*). Although the antibodies gave a different pattern in both cases all the major bands were knocked down except for three minor bands revealed with the N-terminal antibody (see supplemental Fig. 1*C*).

Knocking Down Shank3 Reduces mGluR5 Expression—It has been proposed that Shank3 plays an important role in assem-

bling the PSD and in forming excitatory synapses via its multiple protein-protein interactions (1, 10). Accordingly, we examined the effect of Shank3 knockdown on the protein composition of excitatory synapses using total lysates and synaptosomes from hippocampal cultures infected with shShank3 or shCtrl. Immunoblotting with anti-Shank3 antibody confirmed a strong reduction in Shank3 protein in the synaptosomal fraction of shShank3-infected neurons (Fig. 1, *C* and *D*). Immunoblotting for other glutamate receptors, scaffold proteins, and signaling molecules indicated that there was a significant reduction of mGluR5 in shShank3-infected hippocampal neurons, both in the total lysate and in the synaptosomal fraction (mean ± S.E. for normalized intensity in the total lysate, 0.58 ± 0.03; in the synaptosomal fraction, 0.37 ± 0.05, $p < 0.01$, Student's *t* test). Thus, the level of mGluR5, which binds directly to Shank3 (12), was reduced in shShank3-infected hippocampal neurons. In the same preparations, we detected no significant difference in the abundance of a number of other proteins that are known to be associated with synapses and/or the PSD, including NMDA and AMPA receptors, PSD-95 and IRSp53 (Fig. 1, *C* and *D*). Also unchanged were the total levels of GKAP and Homer scaffold proteins, which can interact directly with Shank3 (11, 12). The reduction in mGluR5 was not dependent on the decrease in mRNA expression as measured by RT-PCR (Fig. 1*A*).

In contrast to the drastic decrease in numbers of Shank3 clusters, the numbers of synaptophysin and PSD-95 clusters were not modified by shShank3 treatment (Fig. 2, *A* and *B*). We previously showed that the inhibition of *Shank3* expression by transfected shRNA in hippocampal neurons reduces dendritic spine numbers (1). Here, we confirm the reduction in spine numbers from 4.9 ± 1.0 spines for 10-μm dendrites in shCtrl-infected neurons to 3.1 ± 0.2 spines/10-μm dendrite in neurons infected with shShank3 (Fig. 2*C*). Spine width and length were also significantly reduced and increased, respectively, in neurons infected with shShank3, suggesting that the remaining spines are smaller and more immature (Fig. 2*D*).

Knockdown of Shank3 Alters the mGluR5 Pathway—The activation of group I mGluRs can lead to a form of long-term depression (mGluR-LTD) that requires rapid translation of pre-existing dendritic mRNA and involves several signaling molecules including ERK1/2 and CREB (36). We investigated the effect of DHPG, the agonist of group I mGluRs, on the relevant signaling pathway by measuring the phosphorylation of ERK1/2 and CREB in response to stimulation of the neurons with DHPG.

shShank3 infection impaired ERK1/2 and CREB phosphorylation induced in neurons stimulated with 100 μM DHPG; KCl depolarization or NMDA stimulation had no such effect (Fig. 3, *A* and *B*). The reduction in DHPG-induced ERK1/2 phosphorylation in the shShank3-transfected neurons was rescued by overexpression of shShank3-resistant Shank3 (Shank3r, see also Fig. 4*A*) (Fig. 3, *C* and *D*). The reduction in DHPG-induced ERK1/2 phosphorylation in these neurons could also be rescued by the overexpression of full-length mGluR5 (data not shown). However, the overexpression of two shShank3-resistant Shank3 mutants, Shank3R87Cr and Shank3InsGr (Fig. 4*A*), which have been found in patients with autism (6) was not

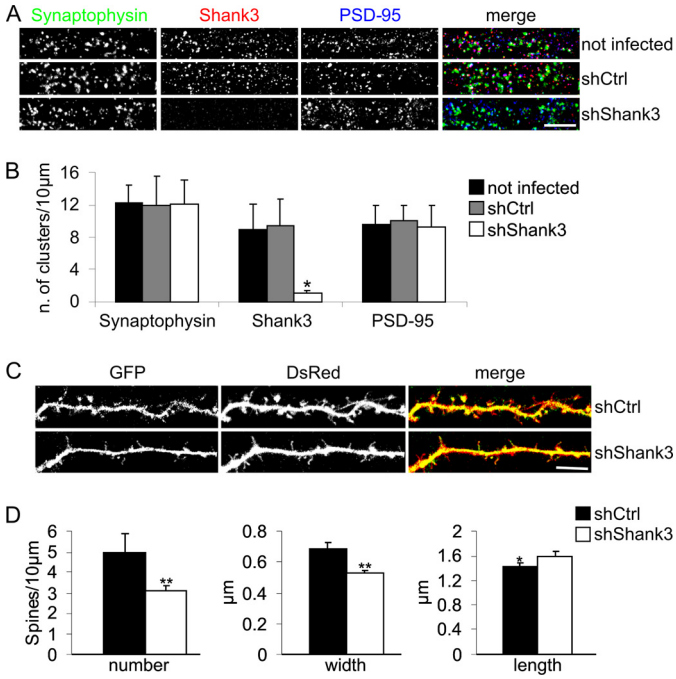

FIGURE 2. *A*, confocal microscopy images of hippocampal neurons infected or not at 7 DIV with a lentivirus expressing shShank3 or shCtrl and stained after 1 week with antibodies specific for Shank3, synaptophysin, and PSD-95 (as indicated *above* the panels). *Scale bar* = 5 μm. *B*, histogram showing mean ± S.E. for four independent experiments, of numbers of Shank3, synaptophysin, and PSD-95 clusters in hippocampal neurons infected with lentivirus expressing shShank3 or shCtrl; at least five neurons were considered for each experiment. The number of Shank3 clusters was significantly lower in the shShank3-infected neurons than in uninfected and shCtrl-infected neurons; *, $p < 0.01$, Student's *t* test. *C*, confocal microscopy images showing dendritic spine morphology in hippocampal neurons infected with shShank3. Hippocampal neurons at 7 DIV were transfected with GFP-containing shCtrl or shShank3 cDNAs, plus DsRed-expressing cDNA. After a week, neurons were fixed and stained for GFP and DsRed. *D*, quantification of number (per 10 μm), length, and width of dendritic spines (± S.E.). Over 14 transfected neurons from four independent experiments were measured for each transfection. Dendritic spine number, length, and width were significantly different in the shShank3-transfected and shCtrl-transfected neurons; **, $p < 0.05$; *, $p < 0.01$, Student's *t* test. *Scale bar* = 10 μm.

able to rescue the ERK1/2 phosphorylation induced by 100 μM DHPG (Fig. 4, *B* and *C*).

To further investigate whether Shank3 deficiency affects synaptic transmission at glutamatergic synapses, we recorded mEPSCs in pyramidal-like cells in shShank3- and shCtrl-treated cultures. Knockdown of Shank3 expression strongly reduced the frequency of mEPSCs, but neither their amplitude nor their time course were affected (Fig. 5, *A–F*). The observed reduction in mEPSC frequency in shShank3-treated cultures is consistent with the reported increase in mEPSC frequency when Shank3 is overexpressed in aspiny cerebellar neurons (1). The reduction in mEPSC frequency in our cultures could be prevented by transfection of shShank3-treated neurons with the shShank3-resistant form of Shank3 (Fig. 5, *G–I*), confirming the specificity of shShank3 treatment.

Activation of mGluR5 could lead to a postsynaptic LTD that is mediated by reduced synaptic expression of AMPA receptors (37, 38). To investigate the functional consequences of Shank3 deficiency for mGluR5-dependent synaptic plasticity, we stimulated shShank3- and shCtrl-treated cultures with 100 μM DHPG. As previously reported for uninfected cultured neurons

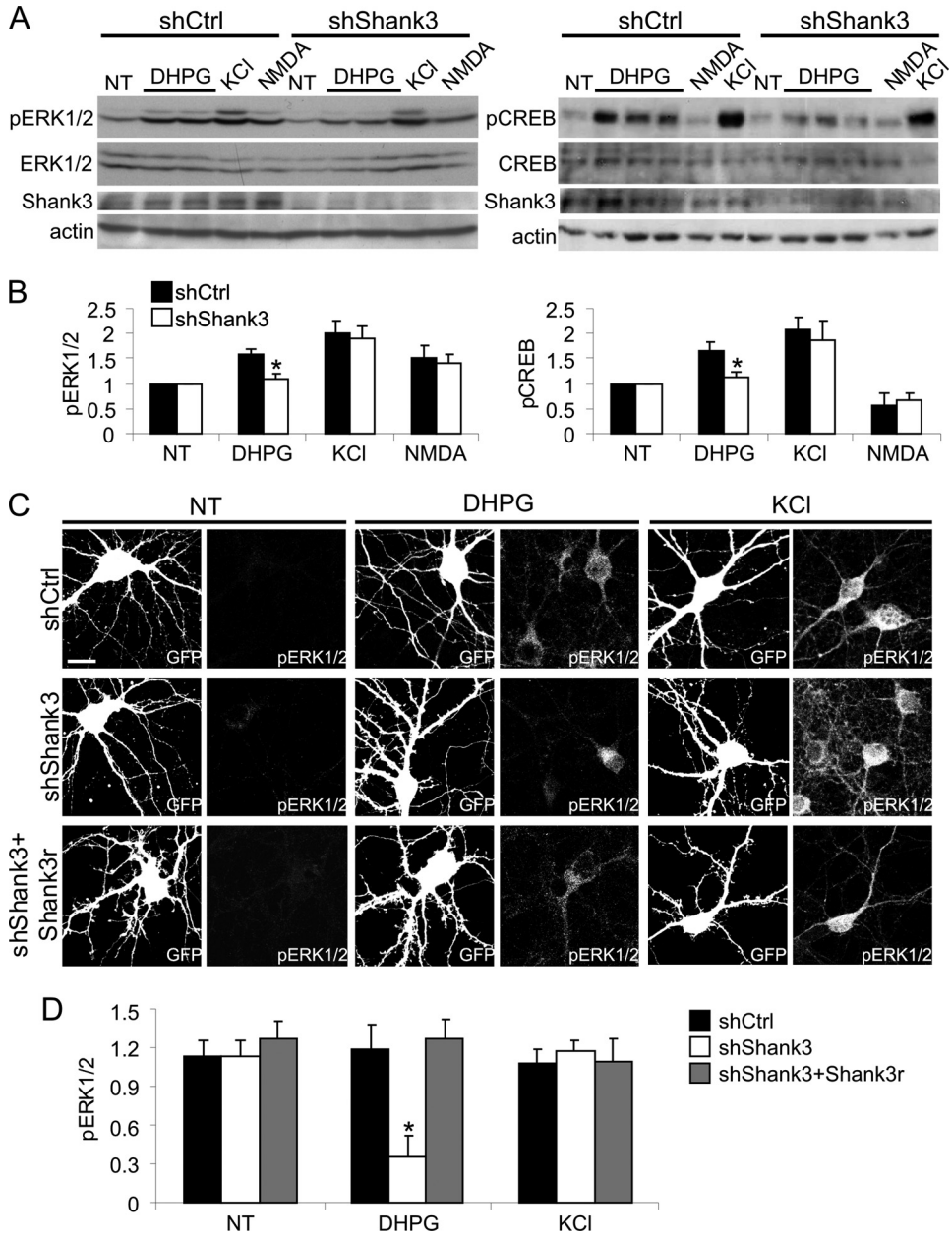

FIGURE 3. **Knockdown of Shank3 alters the mGluR5 pathway.** *A*, Western blot of hippocampal neurons infected at 7 DIV with shCtrl or shShank3. After 1 week, neurons were treated with 100 μM DHPG, 100 μM NMDA, or 50 mM KCl for 30 min, as indicated *above* the panels, and analyzed Shank3, pERK1/2, ERK1/2, pCREB, and CREB expression, as indicated on the *left* of the panels. *B*, histogram showing mean ± S.E., for five independent experiments, of pERK1/2 and pCREB levels (normalized against total ERK and CREB and untreated control (*NT*) values). The levels of pERK1/2 and pCREB were significantly lower in the shShank3-infected neurons than in the shCtrl-infected neurons after DHPG treatment; *, $p < 0.01$, Student's *t* test. *C*, confocal microscopy images of hippocampal neurons transfected at 7 DIV with shCtrl, shShank3, or shShank3 plus Shank3r, as indicated on the *left side* of the panels, and treated on 14 DIV with 100 μM DHPG or 50 mM KCl, as indicated *above* the panels (*NT*, untreated). The neurons were fixed and stained for GFP and pERK1/2. *D*, histogram showing mean ± S.E. values for pERK1/2 signals in each condition of transfection and treatment quantified as described under "Experimental Procedures." The level of pERK1/2 after DHPG treatment was significantly lower in the shShank3-transfected neurons than in the shCtrl- and shShank3 plus Shank3r-transfected neurons; *, $p < 0.05$, Student's *t* test. *Scale bar* = 20 μm.

(29), DHPG induced LTD in the frequency of mEPSC in neurons infected with the control lentivirus. However, LTD was impaired when expression of Shank3 was knocked down (Fig. 6, *A–D*). We also found that shShank3 treatment affected DHPG-induced down-regulation in the number of GluR1-immunoreactive clusters on the plasma membranes of dendrites (Fig. 6, *E* and *F*); a similar down-regulation has been reported for uninfected cultured neurons (29). Furthermore, the density of GluR1-immunoreactive clusters under basal conditions, *i.e.* in neurons not treated with DHPG, was lower in shShank3-treated cultures than in controls. This finding corroborates the observed reduction in the frequency of mEPSCs in shShank3-treated cultures under basal conditions.

Knockdown of Shank3 Impairs DHPG-induced Modulation of Neuronal Network Activity—To investigate the functional effects of Shank3 deficiency at the neural network level, we performed multisite recordings of neuronal activity using multielectrode arrays (Fig. 7). No difference between shShank3-

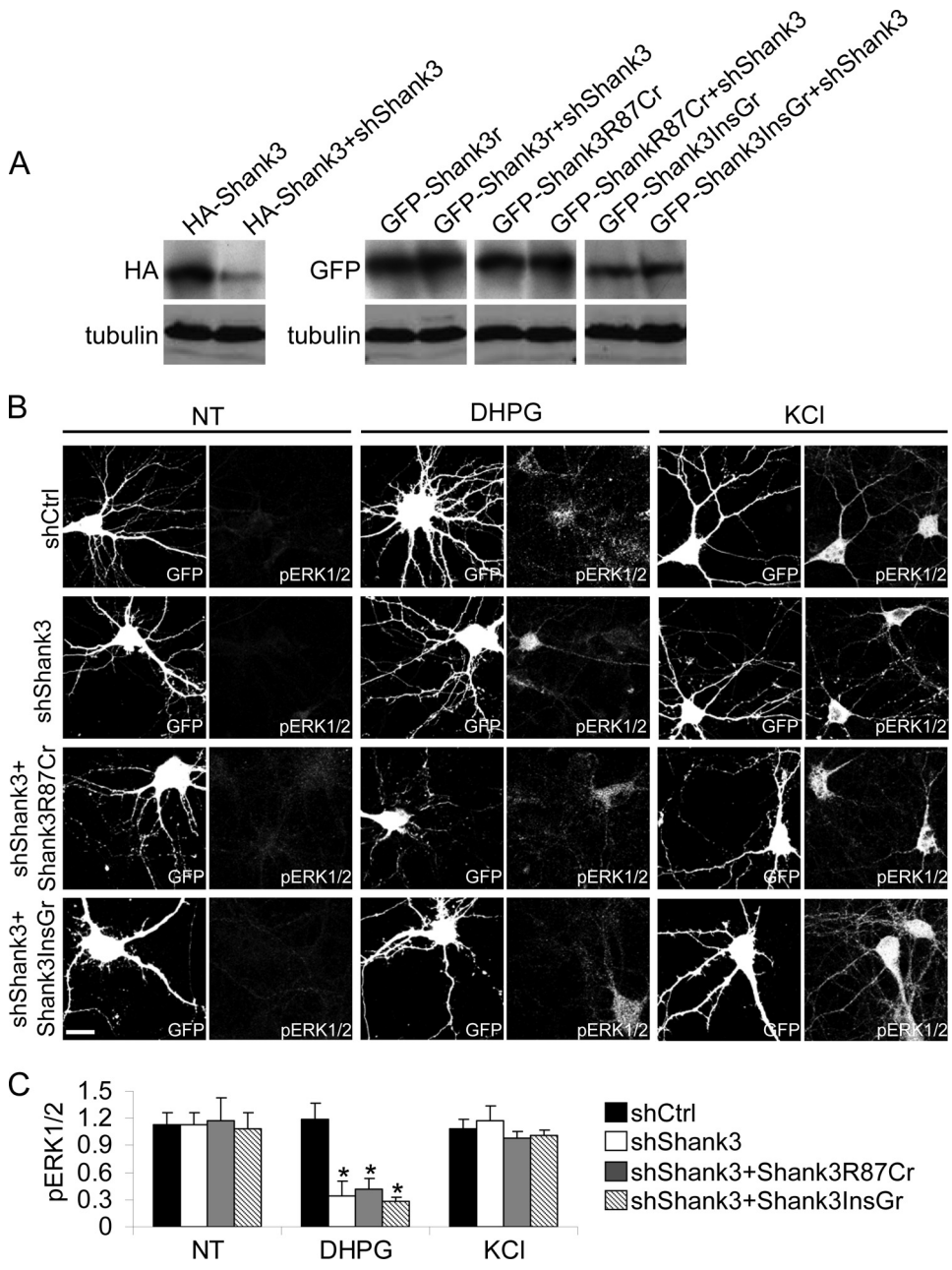

FIGURE 4. **Shank3 mutations found in autistic patients do not rescue shShank3-induced defects in the mGluR5 pathway.** *A*, Western blot of COS-7 cells transfected with HA-Shank3, GFP-Shank3r, GFP-Shank3R87Cr, or GFP-Shank3InsGr plus or minus shShank3, as indicated *above* the panels, and analyzed with anti-HA, anti-GFP, or anti-tubulin antibodies. *B*, confocal microscopy images of hippocampal neurons transfected at 7 DIV with shShank3 + Shank3R87Cr or shShank3 + Shank3InsGr, as indicated on the *left side* of the panels, and treated or not at 14 DIV with 100 μM DHPG or 50 mM KCl, as indicated *above* the panels; the cells were fixed and stained for GFP and pERK1/2. *C*, histogram showing mean ± S.E. values for pERK1/2 in each condition of transfection and treatment quantified as described under "Experimental Procedures." The level of pERK1/2 was significantly lower after DHPG treatment in the shShank3-, shShank3 + Shank3R87Cr-, and shShank3 + Shank3InsGr-transfected neurons than in the shCtrl-transfected neurons; *, $p < 0.05$, Student's *t* test. *Scale bar* = 20 μm.

and shCtrl-treated cultures was detected under basal conditions for any of the parameters of network activity evaluated (Fig. 7*A*, *left panels*, two-way ANOVA, $p > 0.05$). However, DHPG-induced modulation of network activity was more prominent in shCtrl- than in shShank3-treated cultures. In terms of the total spiking rate in all active channels, there was a tendency, albeit not significant, toward lower activity in shShank3-treated cultures (Fig. 7*B*). However, the dose-dependent up-regulation of the number of bursts and spikes out-of-bursts by DHPG was significantly greater in control than in shShank3-treated cultures (Fig. 7, *C* and *E*). Also, there was no DHPG-induced reduction in the spiking frequency within bursts after knockdown of Shank3 (Fig. 7*D*).

Restoration of Frequency of mEPSCs and DHPG-induced Phosphorylation of ERK1/2 in shShank3-treated Cultured Hippocampal Neurons by the Allosteric mGluR5 Agonist CDPPB—To investigate whether the decrease in DHPG-induced ERK1/2 phosphorylation and mEPSC frequency due to reduction of mGluR5 protein expression in shShank3-treated cultures can be pharmacologically rescued, we augmented the activity of mGluR5 using CDPPB as an allosteric positive modulator of this receptor. Overnight treatment with CDPPB restored the

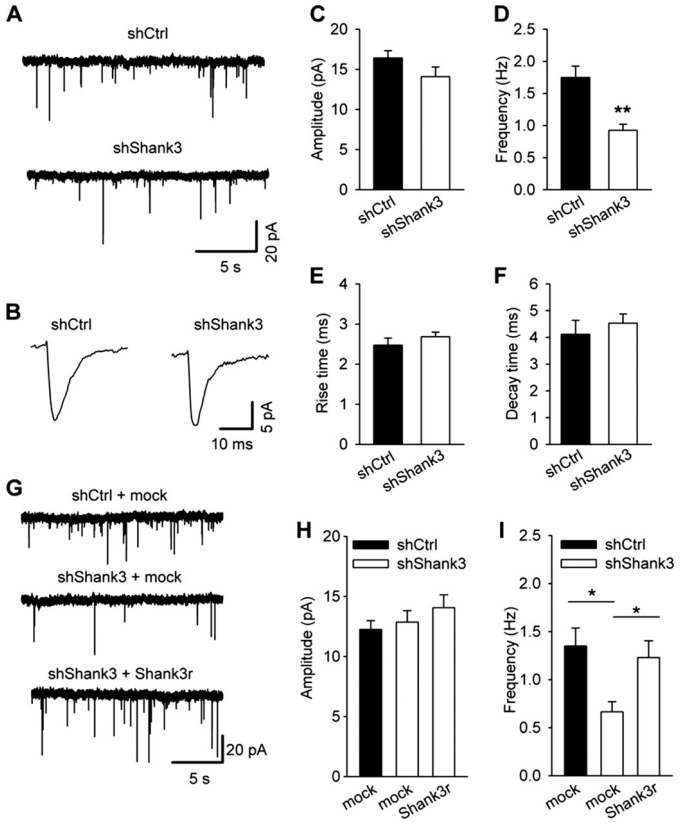

FIGURE 5. **Knockdown of Shank3 expression reduces the frequency of mEPSCs in cultured hippocampal neurons, whereas reintroduction of shShank3-resistant Shank3 restores the frequency of mEPSCs.** *A*, representative mEPSCs recorded on 14 DIV from control neurons (*shCtrl*) and after knockdown of Shank3 (*shShank3*), at a holding potential of −60 mV in the presence of 0.5 μM TTX and 50 μM picrotoxin. *B*, averaged mEPSCs from a control neuron (*left*) and from a shShank3-treated neuron (*right*). *C-F*, summary histograms of mEPSC parameters in control ($n = 16$) and shShank3-treated ($n = 19$) neurons. Data are from seven culture preparations. There is no significant difference in the mEPSC amplitude, rise, or decay time. The frequency of mEPSCs in shShank3-treated neurons is significantly decreased as compared with control neurons; **, $p < 0.005$; Student's *t* test). *G*, representative mEPSCs recorded on 14 DIV from control neurons (*shCtrl* + *mock*), after knockdown of Shank3 (*shShank3* + *mock*) at 8 DIV, and after transfection of Shank3 knocked-down neurons with shShank3-resistant Shank3 at 11 DIV (*shShank3* + *Shank3r*). *H* and *I*, summary histograms of the amplitude (H) and frequency (*I*) of mEPSCs in shCtrl + mock ($n = 12$ cells), shShank3 + mock ($n = 11$ cells), and shShank3 + Shank3r ($n = 14$ cells) treated groups. Data are from four independent experiments. ANOVA revealed a difference in frequency between the three groups ($p < 0.01$). The frequency of mEPSCs was decreased in shShank3 + mock-treated neurons (*, $p < 0.05$, Dunn's test) and recovered in shShank3 + Shank3r-treated cells (*, $p < 0.05$, Dunn's test). Data are presented as mean ± S.E.

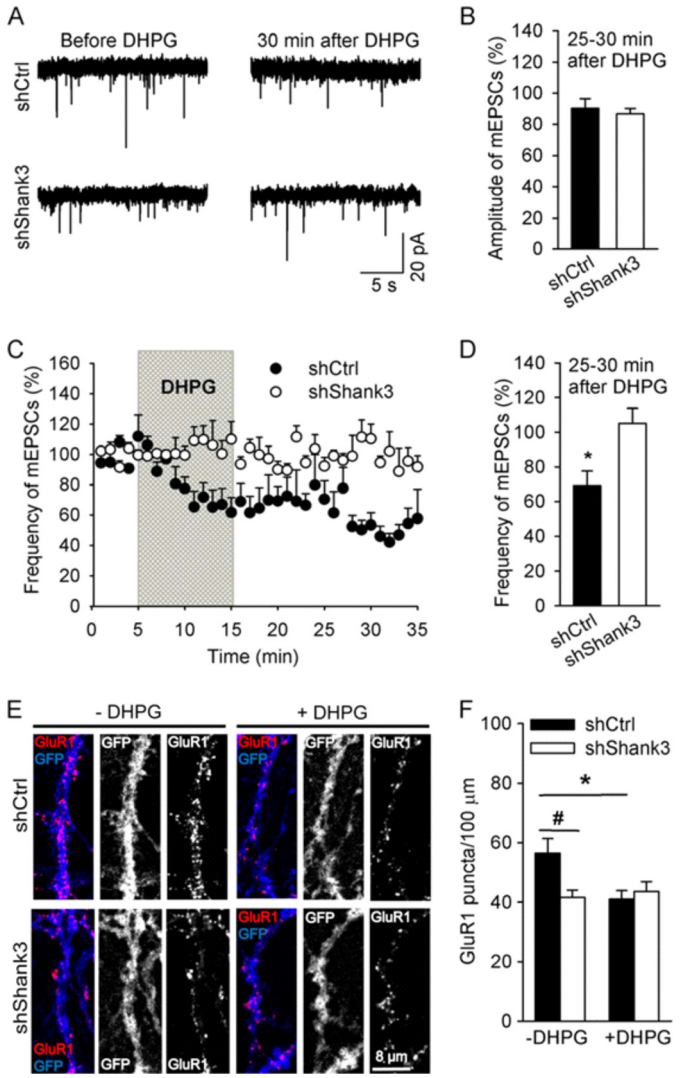

FIGURE 6. **Impairment of DHPG-induced LTD and reduction in cell surface expression of the AMPAR subunit GluR1 in shShank3-treated hippocampal neurons.** *A*, examples of mEPSCs recorded immediately before (*left*) and 30 min after (*right*) DHPG application. Miniature EPSCs were recorded at a holding potential of −60 mV in the presence of 0.5 μM TTX and 50 μM picrotoxin. To isolate mGluR-mediated long term depression, 50 μM APV was co-applied with 100 μM DHPG or applied alone as a control. *A, top*, in shCtrl-treated cultures, 100 μM DHPG elicited a persistent decrease in mEPSC frequency. *A, bottom*, in shShank3-treated neurons, 100 μM DHPG did not induce a decrease in mEPSC frequency. *B*, histogram showing mean ± S.E. % mEPSC amplitude in shCtrl or in shShank3-treated neurons stimulated with DHPG. *C*, effect of DHPG on mEPSC frequency in shCtrl (*black circles*, $n = 7$ neurons) and in shShank3-treated neurons (*gray circles*, $n = 7$ neurons). Data presented are mean ± S.E. from three culture preparations. The frequency of mEPSCs during the first 5 min of recordings (*i.e.* before application of DHPG) was set to 100%. *D*, summary plot showing changes in mean mEPSC frequency 30–35 min after application of DHPG; *, $p < 0.05$, Student's *t* test. *E*, examples of confocal images of cell surface immunostaining of GluR1 in hippocampal neurons at 14 DIV. Neurons were treated with 100 μM DHPG (*+DHPG*) for 10 min, or not treated (*−DHPG*). *E, top*). There is a reduction in cell surface expression of GluR1 in control neurons (*shCtrl*) after DHPG treatment. *E, bottom*, in shShank3-treated neurons, the number of GluR1-immunoreactive clusters on the surface of dendrites was reduced, and treatment with DHPG did not affect the surface expression of GluR1. *F*, summary plot of GluR1 cell surface distribution in shCtrl and shShank3-treated neurons after DHPG treatment. The diagram summarizes data from five culture preparations; #, $p < 0.05$, Student's *t* test; *, $p < 0.05$, paired *t* test. Data are presented as mean ± S.E.

frequency of mEPSCs (Fig. 8, *A* and *B*). Notably, we also found that the DHPG-induced phosphorylation of ERK1/2 in neurons infected with shShank3 was rescued by overnight treatment with CDPPB (Fig. 8, *C* and *D*). These data suggest that the mGluR type I signaling that is altered by the knockdown of Shank3 can be potentially restored by CDPPB.

DISCUSSION

We have studied the role of Shank3 in synapse function to better understand the pathogenesis of the neurological symptoms of patients affected by Phelan-McDermid syndrome (2, 39). For this purpose, we used a specific shRNA to knockdown the expression of the major splice variants of Shank3 in cultured murine neurons. Our immunoblotting study using two differ-

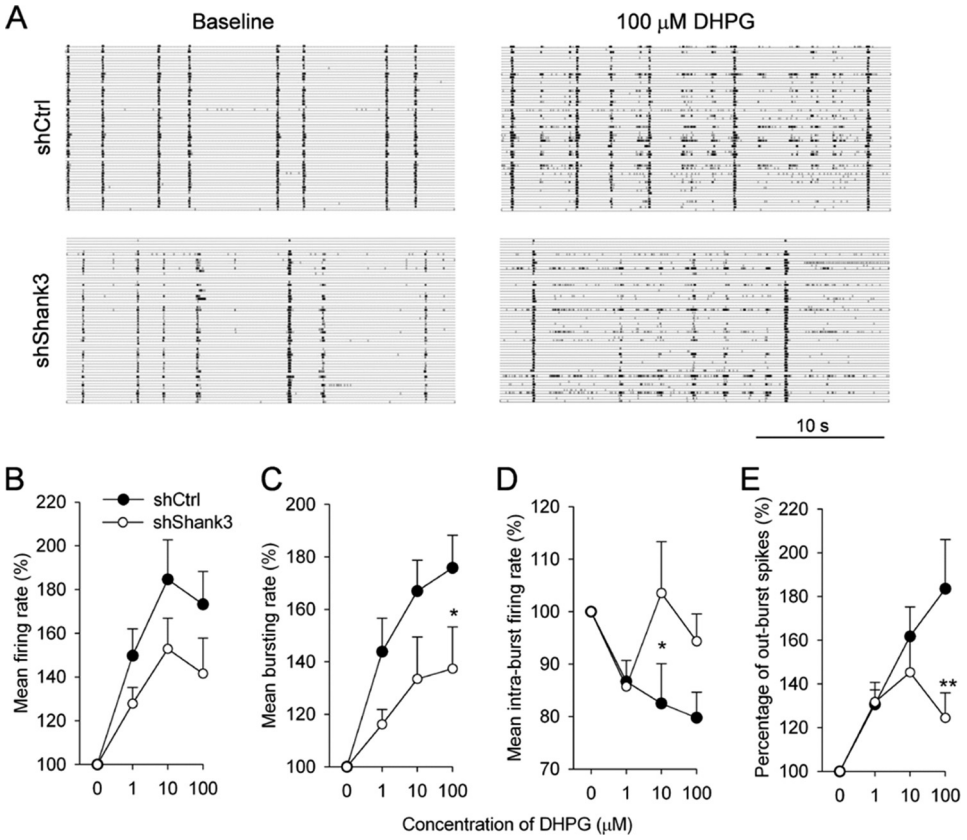

FIGURE 7. **Knockdown of Shank3 impairs DHPG-induced modulation of neuronal network activity.** *A*, representative 60-electrode recordings of activity of cultured mouse neurons before and 5 min after application of 100 μM DHPG. Each *horizontal line* corresponds to one electrode; *short vertical* intervals correspond to detected action potentials. The duration of each recording is 30 s. Following application of 100 μM DHPG, a greater increase in the number of bursts occurs in the shCtrl-treated cultures compared with the shShank3-treated cultures. *B-E*, changes in the mean firing rate (*B*), bursting rate (*C*), intra-burst firing rate (*D*), and percentage of out-burst spikes (*E*) for active electrodes after the application of DHPG to shCtrl- and shShank3-treated cultures. There were no differences between shCtrl- and shShank3-treated groups in baseline activity; therefore, the values of parameters estimated under the baseline condition were set to 100% for each culture. Two-way ANOVA with repeated measures (DHPG concentrations of 1, 10, and 100 μM) revealed a significant effect of DHPG ($p < 0.01$), but not of shShank3 or shShank3 + DHPG on the mean firing rate (*B*). Significant effects of DHPG ($p < 0.01$) and shShank3 ($p = 0.05$) on the mean bursting rate were detected in *C*, and significant effects of shShank3 + DHPG ($p < 0.05$) on the intra-burst firing rate (*D*) and % of out-burst spikes (*E*) were detected. *, $p < 0.05$; **, $p < 0.01$, Holm-Sidak post hoc *t* test, significant differences between shCtrl- ($n = 10$ cultures) and shShank3-treated cultures ($n = 7$ cultures).

ent anti-Shank3 antibodies, one against the N terminus and one against the C terminus, indicated that, at least in neuronal cultures, Shank3 shRNA knocked down all the major Shank3-specific bands. As Wang *et al.* (21) recently described six intragenic promoters that could potentially generate multiple splicing variants coding for several isoforms of Shank3, we cannot exclude that some minor splice variants remain at undetectable levels beyond shSank3 inhibition.

Although the proteins encoded by these three SHANK genes are structurally similar, some evidence suggests that they differ in function, in synapse-targeting properties, and in binding partners. For example, the overexpression of Shank1 induces maturation of dendritic spines without increasing their numbers, whereas the overexpression of Shank3 induces the formation of new synapses and dendritic spines (1, 16). Shank1 targeting to synapses is dependent on the PDZ domain, but the targeting of Shank2 and Shank3 depends on their C-terminal domain, including the sterile α motif domain (24, 40). Shank2 and Shank3 multimerize and form a platform or framework in the PSD that depends on Zn^{2+} binding to the sterile α motif domain (18, 41). In contrast, Shank1 does not bind Zn^{2+}, but forms a large framework complex with Homer in the PSD (19).

The specific function of Shank proteins in dendritic spines is probably related to the fact that all three protein variants bind directly to a number of proteins involved in actin remodeling, such as cortactin, Abp1, IRsP53, and SPIN90 (11, 42–44); they also interact indirectly with actin-remodeling proteins through binding Homer, oligophrenin, and CdC42 (45, 46). Available data suggest that Shank proteins functionally link glutamate receptors to the cytoskeleton, thereby regulating the size and dimensions of excitatory synapses and dendritic spines (47).

Shank2 and -3 can also bind to Ab1 and LAPSER1, two proteins that translocate from the PSD to the nucleus in an activity-dependent manner and induce gene transcription and translation (48, 49). Finally, the fact that simple deletions of either *SHANK3* or *SHANK2*, but not, up to now, *SHANK1*, have been clearly implicated in the pathogenesis of mental retardation, autism and, more recently, schizophrenia, suggest that the three proteins may have different functions that cannot compensate for each other. Thus, it is important to note that we did not observe any type of compensation by the other SHANK member as neither Shank1 nor Shank2 expression increased upon Shank3 knockdown.

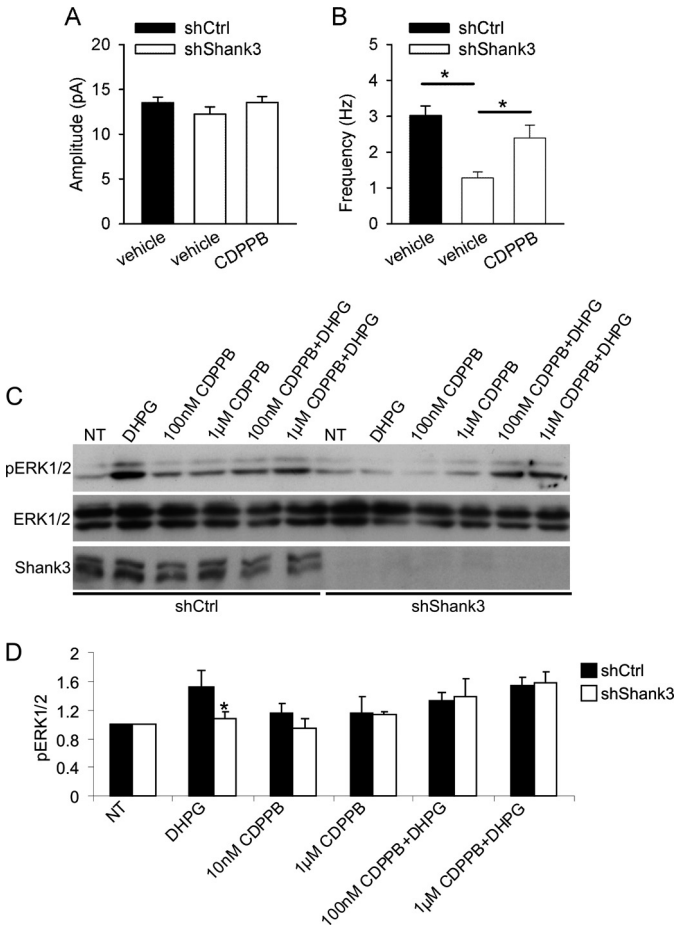

FIGURE 8. **Restoration of frequency of mEPSCs and DHPG-induced phosphorylation of ERK1/2 in shShank3-treated cultured hippocampal neurons by the allosteric mGluR5 agonist CDPPB.** *A* and *B,* neurons were infected with lentiviruses at 8 DIV and treated overnight with 1 μM CDPPB at 13 DIV. On 14 DIV, mEPSCs were recorded at a holding potential of −60 mV in the presence of 0.5 μM TTX and 50 μM picrotoxin. Summary graphs of the amplitude (*A*) and frequency (*B*) of mEPSCs in shCtrl + vehicle ($n = 11$ cells), shShank3 + vehicle ($n = 14$ cells), and shShank3 + CDPPB ($n = 14$ cells)-treated groups. Data are from four culture preparations. The frequency of mEPSCs is significantly decreased in shShank3 + vehicle as compared with shCtrl + vehicle-treated neurons and recovers significantly in shShank3 + CDPPB-treated cells; *, $p \leq 0.05$, Dunn's test. Data are presented as mean ± S.E. *C*, Western blot of hippocampal neurons infected at 7 DIV with shCtrl or shShank3 and treated after 1 week as indicated *above* the panels. The proteins analyzed are indicated to the *left* of the panels. *D,* histogram showing mean ± S.E. for five independent experiments, of ERK1/2 phosphorylation, normalized to total ERK and untreated (*NT*) values. The level of pERK1/2 after DHPG treatment was significantly lower in the shShank3-infected neurons than in the shCtrl-infected neurons; *, $p < 0.01$, Student's *t* test.

We found that knockdown of Shank3 specifically impaired mGluR5 signaling at synapses. In hippocampal neurons knocked down for Shank3, mGluR5 protein, but not its mRNA, is specifically reduced in the total lysate and in the synaptosomes, suggesting that Shank3 is somehow involved in mGluR5 protein stabilization. Previous work has shown that mGluR5 binds directly to Shank3 or indirectly through Homer cross-linking (12). However, because we did not find any change in Homer expression, it is possible that the direct binding of Shank3 to mGluR5 is involved in this phenomenon. Both Shank3 and mGluR5 can be degraded by proteasomes following ubiquitination, suggesting that their interaction can reciprocally modulate their ubiquitination and stabilization (50, 51). However, we did not find any change in Shank3 protein expression in the mGluR5 knock-out mice.[5] Thus, Shank3 might act as a stabilization platform for mGluR5. We also observed a reduction in cell surface expression of GluR1 in shShank3-treated neurons without a reduction in its protein expression. The reduction in GluR1 cell surface expression correlated with the reduced mEPSC frequency. The impaired DHPG-dependent LTD observed in shShank3-treated neurons did not result in any changes in cell surface expression of GluR1, which is down-regulated by DHPG in shCtrl-treated neurons. Our findings that CDPPB, an allosteric mGluR5 agonist, was able to rescue the mEPSC frequency in neurons knocked down for Shank3 suggest that Shank3 regulates AMPA receptor trafficking in an mGluR5-dependent manner. The reduction in cell surface GluR1 expression and in frequency of mEPSCs after knockdown of Shank3 might reflect impairment in activity-dependent synaptic recruitment of AMPA receptors at basal conditions.

Despite the observed reduction in mEPSC frequency and cell surface expression of GluR1-positive clusters in shShank3-treated neurons, our multielectrode recordings did not reveal significant changes in the spiking patterns of neurons under basal conditions. This is not surprising, because the connectivity between cultured neurons is highly redundant. Therefore, despite the differences in synaptic activity between control and Shank3-knockdown neurons in TTX-treated cultures, the composite postsynaptic potentials might well exceed the threshold for spike generation in these cells in the absence of TTX. Application of DHPG to cultured neurons led to a strong increase in the bursting rate, as previously reported for hippocampal slices (52). Importantly, DHPG-induced up-regulation of bursting was reduced in Shank3-knockdown neurons. This result confirms the importance of Shank3 in the regulation of mGluR5-dependent signaling under physiological conditions, *i.e.* in the absence of TTX. It also demonstrates the potential importance of Shank3 in mGluR5 activity-induced shaping of neural network activity.

In a recent analysis of the role of Shank3 mutations when overexpressed in hippocampal neurons, Durand *et al.* (53) showed that all mutations analyzed modify Shank3 functions. Here, we have analyzed two of the mutations studied by Durand *et al.* (their R12C corresponds to our R87C and their Shank3^{STOP} corresponds to our Shank3Ins). Both mutations were shown by Durand *et al.* (53) to affect the ability of Shank3 proteins to increase the dimension of dendritic spines and modify synaptic properties. Interestingly, in our study, the expression of mutated forms of Shank3 that mimic the mutations found in autistic patients was not able to rescue DHPG-dependent ERK1/2 phosphorylation. Thus, reduction in Shank3 expression, which occurs in 22q13/Phelan-McDermid syndrome, and functional mutations in Shank3, which occur in some autistic patients, might both induce alterations in mGluR5 signaling at synapses.

Four recent studies highlight the importance of Shank3 at the molecular and behavioral levels (21–23, 54). Two of them showed that Shank3 heterozygous and homozygous male mice displayed abnormal social behavior, communication pattern,

[5] C. Verpelli and C. Sala, unpublished results.

and learning and memory, as compared with wild-type littermate controls (21, 54). These studies revealed a strong impairment in basal synaptic transmission in CA3-CA1 connections, a reduction in GluR1 clusters and protein levels in the hippocampus, and an alteration in activity-dependent AMPAR synaptic plasticity (21, 54). However, the reduction in mEPSC amplitude and the "compensatory" increase in mEPSC frequency in Shank3 heterozygous mice reported by these authors were not seen in our experiments. Most importantly in this context, it should be noted that in our experiments, in contrast to the other studies, we knocked down all detectable Shank3 splice variants through shRNA treatment; this led to a suppression of Shank3 expression by 70–80% rather than by 50% as in Shank3 heterozygous mice. This could lead to such a strong reduction of mEPSC amplitudes that EPSCs would decrease below the detection limit, resulting in a reduction of mEPSC frequency, as we report here. Another difference is our observation that Shank3 plays a role in LTD induced by the mGluR type 1 agonist, DHPG, whereas Bozdagi and colleagues (54) found that Shank3 heterozygous mice have a normal LTD induced by paired-pulse low-frequency stimulation. In view of our present study, this is not surprising considering the role of Shank3 in regulation of mGluR5 expression and considering that previous studies in mGluR5 knock-out mice have also shown normal paired-pulse low-frequency stimulation-induced LTD (55), but impaired DHPG-induced LTD (56).

Peça *et al.* (22) have instead reported that mice genetically deleted of two major Shank3 splice variants exhibit self-injurious repetitive grooming and deficits in social interaction and these behavioral defects are caused by major alteration in the striatal synapses and cortico-striatal circuits, but not in the hippocampus. Thus, it is possible that the remaining Shank3 splice variant(s) might be sufficient to maintain normal synapse function and structure in the hippocampus. Paradoxically, the remaining Shank3 protein described by Bangash *et al.* (23), which misses the C-terminal fragment, has a gain-of-function phenotype by reducing the NR1 subunit of NMDA receptors specifically at synapses, but not affecting synaptic AMPAR function and composition. Although this pathway should obviously also be investigated *in vivo*, our data strongly suggest nevertheless that knocking down all the major Shank3 splice variants strongly affects the expression of mGluR5 receptor at the synapses.

The mGluR5 receptor plays a major role in synaptic plasticity (57). It has been clearly demonstrated that antagonism or genetic deletion of mGluR5 impairs both acquisition and extinction of hippocampal-dependent learning tasks, such as the radial arm maze and the Morris water maze, by impairing both the late phase of hippocampal long term potentiation and mGluR-dependent LTD (58–60). The occurrence of mGluR-dependent LTD in CA1 relies on activation of both ERK and PI3K-mTOR pathways (36, 61). A role for mGluR-LTD has been demonstrated for the formation of object recognition memory (62, 63).

The existence of a link between mGluR-LTD and cognitive disease is suggested by the finding that both hippocampal and cerebellar mGluR-LTD are altered in fragile X syndrome, a mouse model of mental retardation and autism that has led to the development of novel therapeutics for this syndrome that act on mGluR5 (64). In contrast to our finding in Shank3-knockdown neurons, mGluR-LTD is enhanced in the fragile X syndrome mouse model (65). This enhancement occurs because, in the absence of fragile X mental retardation protein, as in fragile X syndrome, there is a loss of steady-state translational suppression that leads to increased protein levels of fragile X mental retardation protein targeting specific mRNAs, such as those coding for activity-regulated cytoskeleton-associated protein that may enhance the magnitude of LTD (66).

Notably, the use of mGluR5 antagonists or genetic reduction of mGluR5 (in mice that are heterozygous for mGluR5) can reverse multiple phenotypes in mice deficient in *FMR1*, a gene encoding the fragile X mental retardation protein; these phenotypes include increased dendritic spine density and deficits in experience-dependent plasticity in the visual cortex and hippocampal-dependent learning (67, 68).

Based on this finding, we tested whether the reduced mGluR5 activity in Shank3-knockdown neurons can be rescued by an allosteric agonist of mGluR5, such as CDPPB (69, 70), and found that both ERK1/2 phosphorylation and mEPSC frequency were rescued by overnight treatment with CDPPB. CDPPB has been shown to be brain-penetrant and to reverse amphetamine-induced locomotor activity and amphetamine-induced deficits in prepulse inhibition in rats (70), two models that are sensitive to antipsychotic drug treatment. These results demonstrate that positive allosteric modulation of mGluR5 produces behavioral effects and suggest that mGluR5 activity could be envisaged as a potential therapeutic target. Therefore, these findings open new possibilities for the pharmacological treatment of patients affected by Shank3 gene deletion and mutation.

Acknowledgment—We thank N. Tonna for some preliminary data.

REFERENCES

1. Roussignol, G., Ango, F., Romorini, S., Tu, J. C., Sala, C., Worley, P. F., Bockaert, J., and Fagni, L. (2005) *J. Neurosci.* **25,** 3560–3570
2. Bonaglia, M. C., Giorda, R., Borgatti, R., Felisari, G., Gagliardi, C., Selicorni, A., and Zuffardi, O. (2001) *Am. J. Hum. Genet.* **69,** 261–268
3. Wilson, H. L., Crolla, J. A., Walker, D., Artifoni, L., Dallapiccola, B., Takano, T., Vasudevan, P., Huang, S., Maloney, V., Yobb, T., Quarrell, O., and McDermid, H. E. (2008) *Eur. J. Hum. Genet.* **16,** 1301–1310
4. Wilson, C. A., Doms, R. W., and Lee, V. M. (2003) *J. Neurosci. Res.* **74,** 361–369
5. Bonaglia, M. C., Giorda, R., Mani, E., Aceti, G., Anderlid, B. M., Baroncini, A., Pramparo, T., and Zuffardi, O. (2006) *J. Med. Genet.* **43,** 822–828
6. Durand, C. M., Betancur, C., Boeckers, T. M., Bockmann, J., Chaste, P., Fauchereau, F., Nygren, G., Rastam, M., Gillberg, I. C., Anckarsäter, H., Sponheim, E., Goubran-Botros, H., Delorme, R., Chabane, N., Mouren-Simeoni, M. C., de Mas, P., Bieth, E., Rogé, B., Héron, D., Burglen, L., Gillberg, C., Leboyer, M., and Bourgeron, T. (2007) *Nat. Genet.* **39,** 25–27
7. Moessner, R., Marshall, C. R., Sutcliffe, J. S., Skaug, J., Pinto, D., Vincent, J., Zwaigenbaum, L., Fernandez, B., Roberts, W., Szatmari, P., and Scherer, S. W. (2007) *Am. J. Hum. Genet.* **81,** 1289–1297
8. Delahaye, A., Toutain, A., Aboura, A., Dupont, C., Tabet, A. C., Benzacken, B., Elion, J., Verloes, A., Pipiras, E., and Drunat, S. (2009) *Eur. J. Med. Genet.* **52,** 328–332
9. Gauthier, J., Spiegelman, D., Piton, A., Lafrenière, R. G., Laurent, S., St-Onge, J., Lapointe, L., Hamdan, F. F., Cossette, P., Mottron, L., Fombonne, E., Joober, R., Marineau, C., Drapeau, P., and Rouleau, G. A. (2009) *Am. J. Med. Genet. B Neuropsychiatr. Genet.* **150,** 421–424
10. Sheng, M., and Kim, E. (2000) *J. Cell Sci.* **113,** 1851–1856
11. Naisbitt, S., Kim, E., Tu, J. C., Xiao, B., Sala, C., Valtschanoff, J., Weinberg,

R. J., Worley, P. F., and Sheng, M. (1999) *Neuron* **23,** 569–582
12. Tu, J. C., Xiao, B., Naisbitt, S., Yuan, J. P., Petralia, R. S., Brakeman, P., Doan, A., Aakalu, V. K., Lanahan, A. A., Sheng, M., and Worley, P. F. (1999) *Neuron* **23,** 583–592
13. Boeckers, T. M., Winter, C., Smalla, K. H., Kreutz, M. R., Bockmann, J., Seidenbecher, C., Garner, C. C., and Gundelfinger, E. D. (1999) *Biochem. Biophys. Res. Commun.* **264,** 247–252
14. Sala, C., Piëch, V., Wilson, N. R., Passafaro, M., Liu, G., and Sheng, M. (2001) *Neuron* **31,** 115–130
15. Sala, C., Futai, K., Yamamoto, K., Worley, P. F., Hayashi, Y., and Sheng, M. (2003) *J. Neurosci.* **23,** 6327–6337
16. Sala, C., Roussignol, G., Meldolesi, J., and Fagni, L. (2005) *J. Neurosci.* **25,** 4587–4592
17. Hung, A. Y., Futai, K., Sala, C., Valtschanoff, J. G., Ryu, J., Woodworth, M. A., Kidd, F. L., Sung, C. C., Miyakawa, T., Bear, M. F., Weinberg, R. J., and Sheng, M. (2008) *J. Neurosci.* **28,** 1697–1708
18. Baron, M. K., Boeckers, T. M., Vaida, B., Faham, S., Gingery, M., Sawaya, M. R., Salyer, D., Gundelfinger, E. D., and Bowie, J. U. (2006) *Science* **311,** 531–535
19. Hayashi, M. K., Tang, C., Verpelli, C., Narayanan, R., Stearns, M. H., Xu, R. M., Li, H., Sala, C., and Hayashi, Y. (2009) *Cell* **137,** 159–171
20. Maunakea, A. K., Nagarajan, R. P., Bilenky, M., Ballinger, T. J., D'Souza, C., Fouse, S. D., Johnson, B. E., Hong, C., Nielsen, C., Zhao, Y., Turecki, G., Delaney, A., Varhol, R., Thiessen, N., Shchors, K., Heine, V. M., Rowitch, D. H., Xing, X., Fiore, C., Schillebeeckx, M., Jones, S. J., Haussler, D., Marra, M. A., Hirst, M., Wang, T., and Costello, J. F. (2010) *Nature* **466,** 253–257
21. Wang, X., McCoy, P. A., Rodriguiz, R. M., Pan, Y., Je, H. S., Roberts, A. C., Kim, C. J., Berrios, J., Colvin, J. S., Bousquet-Moore, D., Lorenzo, I., Wu, G., Weinberg, R. J., Ehlers, M. D., Philpot, B. D., Beaudet, A. L., Wetsel, W. C., and Jiang, Y. H. (2011) *Hum. Mol. Genet.* **20,** 3093–3108
22. Peça, J., Feliciano, C., Ting, J. T., Wang, W., Wells, M. F., Venkatraman, T. N., Lascola, C. D., Fu, Z., and Feng, G. (2011) *Nature* **472,** 437–442
23. Bangash, M. A., Park, J. M., Melnikova, T., Wang, D., Jeon, S. K., Lee, D., Syeda, S., Kim, J., Kouser, M., Schwartz, J., Cui, Y., Zhao, X., Speed, H. E., Kee, S. E., Tu, J. C., Hu, J. H., Petralia, R. S., Linden, D. J., Powell, C. M., Savonenko, A., Xiao, B., and Worley, P. F. (2011) *Cell* **145,** 758–772
24. Romorini, S., Piccoli, G., Jiang, M., Grossano, P., Tonna, N., Passafaro, M., Zhang, M., and Sala, C. (2004) *J. Neurosci.* **24,** 9391–9404
25. Dityatev, A., Dityateva, G., and Schachner, M. (2000) *Neuron* **26,** 207–217
26. Seeburg, D. P., and Sheng, M. (2008) *J. Neurosci.* **28,** 6583–6591
27. Beri, S., Tonna, N., Menozzi, G., Bonaglia, M. C., Sala, C., and Giorda, R. (2007) *J. Neurochem.* **101,** 1380–1391
28. Verpelli, C., Piccoli, G., Zanchi, A., Gardoni, F., Huang, K., Brambilla, D., Di Luca, M., Battaglioli, E., and Sala, C. (2010) *J. Neurosci.* **30,** 5830–5842
29. Moult, P. R., Gladding, C. M., Sanderson, T. M., Fitzjohn, S. M., Bashir, Z. I., Molnar, E., and Collingridge, G. L. (2006) *J. Neurosci.* **26,** 2544–2554
30. Piccoli, G., Verpelli, C., Tonna, N., Romorini, S., Alessio, M., Nairn, A. C., Bachi, A., and Sala, C. (2007) *J. Proteome Res.* **6,** 3203–3215
31. Cancedda, L., Fiumelli, H., Chen, K., and Poo, M. M. (2007) *J. Neurosci.* **27,** 5224–5235
32. Blau, A., Neumann, T., Ziegler, C., and Benfenati, F. (2009) *J. Biosci.* **34,** 59–69
33. Bologna, L. L., Nieus, T., Tedesco, M., Chiappalone, M., Benfenati, F., and Martinoia, S. (2010) *Neuroscience* **165,** 692–704
34. Maccione, A., Gandolfo, M., Massobrio, P., Novellino, A., Martinoia, S., and Chiappalone, M. (2009) *J. Neurosci. Methods* **177,** 241–249
35. Pasquale, V., Martinoia, S., and Chiappalone, M. (2010) *J. Comput. Neurosci.* **29,** 213–229
36. Gallagher, S. M., Daly, C. A., Bear, M. F., and Huber, K. M. (2004) *J. Neurosci.* **24,** 4859–4864
37. Collingridge, G. L., Peineau, S., Howland, J. G., and Wang, Y. T. (2010) *Nat. Rev. Neurosci.* **11,** 459–473
38. Lüscher, C., and Huber, K. M. (2010) *Neuron* **65,** 445–459
39. Wilson, H. L., Wong, A. C., Shaw, S. R., Tse, W. Y., Stapleton, G. A., Phelan, M. C., Hu, S., Marshall, J., and McDermid, H. E. (2003) *J. Med. Genet.* **40,** 575–584
40. Boeckers, T. M., Liedtke, T., Spilker, C., Dresbach, T., Bockmann, J., Kreutz, M. R., and Gundelfinger, E. D. (2005) *J. Neurochem.* **92,** 519–524
41. Grabrucker, A. M., Knight, M. J., Proepper, C., Bockmann, J., Joubert, M., Rowan, M., Nienhaus, G. U., Garner, C. C., Bowie, J. U., Kreutz, M. R., Gundelfinger, E. D., and Boeckers, T. M. (2011) *EMBO J.* **30,** 569–581
42. Bockmann, J., Kreutz, M. R., Gundelfinger, E. D., and Böckers, T. M. (2002) *J. Neurochem.* **83,** 1013–1017
43. Qualmann, B., Boeckers, T. M., Jeromin, M., Gundelfinger, E. D., and Kessels, M. M. (2004) *J. Neurosci.* **24,** 2481–2495
44. Kim, S. M., Choi, K. Y., Cho, I. H., Rhy, J. H., Kim, S. H., Park, C. S., Kim, E., and Song, W. K. (2009) *J. Neurochem.* **109,** 1106–1117
45. Govek, E. E., Newey, S. E., Akerman, C. J., Cross, J. R., Van der Veken, L., and Van Aelst, L. (2004) *Nat. Neurosci.* **7,** 364–372
46. Shiraishi-Yamaguchi, Y., Sato, Y., Sakai, R., Mizutani, A., Knöpfel, T., Mori, N., Mikoshiba, K., and Furuichi, T. (2009) *BMC Neurosci.* **10,** 25
47. Boeckers, T. M., Bockmann, J., Kreutz, M. R., and Gundelfinger, E. D. (2002) *J. Neurochem.* **81,** 903–910
48. Proepper, C., Johannsen, S., Liebau, S., Dahl, J., Vaida, B., Bockmann, J., Kreutz, M. R., Gundelfinger, E. D., and Boeckers, T. M. (2007) *EMBO J.* **26,** 1397–1409
49. Schmeisser, M. J., Grabrucker, A. M., Bockmann, J., and Boeckers, T. M. (2009) *J. Biol. Chem.* **284,** 29146–29157
50. Moriyoshi, K., Iijima, K., Fujii, H., Ito, H., Cho, Y., and Nakanishi, S. (2004) *Proc. Natl. Acad. Sci. U.S.A.* **101,** 8614–8619
51. Gong, Y., Lippa, C. F., Zhu, J., Lin, Q., and Rosso, A. L. (2009) *Brain Res.* **1292,** 191–198
52. Quitsch, A., Berhörster, K., Liew, C. W., Richter, D., and Kreienkamp, H. J. (2005) *J. Neurosci.* **25,** 479–487
53. Durand, C. M., Perroy, J., Loll, F., Perrais, D., Fagni, L., Bourgeron, T., Montcouquiol, M., and Sans, N. (2011) *Mol. Psychiatry* doi: 10.1038/mp.2011.57
54. Bozdagi, O., Sakurai, T., Papapetrou, D., Wang, X., Dickstein, D. L., Takahashi, N., Kajiwara, Y., Yang, M., Katz, A. M., Scattoni, M. L., Harris, M. J., Saxena, R., Silverman, J. L., Crawley, J. N., Zhou, Q., Hof, P. R., and Buxbaum, J. D. (2010) *Mol. Autism* **1,** 15
55. Volk, L. J., Daly, C. A., and Huber, K. M. (2006) *J. Neurophysiol.* **95,** 2427–2438
56. Huber, K. M., Roder, J. C., and Bear, M. F. (2001) *J. Neurophysiol.* **86,** 321–325
57. Simonyi, A., Schachtman, T. R., and Christoffersen, G. R. (2010) *Eur. J. Pharmacol.* **639,** 17–25
58. Lu, Y. M., Jia, Z., Janus, C., Henderson, J. T., Gerlai, R., Wojtowicz, J. M., and Roder, J. C. (1997) *J. Neurosci.* **17,** 5196–5205
59. Naie, K., and Manahan-Vaughan, D. (2004) *Cereb. Cortex* **14,** 189–198
60. Manahan-Vaughan, D., and Braunewell, K. H. (2005) *Cereb. Cortex* **15,** 1703–1713
61. Hough, C. D., Woods, D. F., Park, S., and Bryant, P. J. (1997) *Genes Dev.* **11,** 3242–3253
62. Jo, J., Ball, S. M., Seok, H., Oh, S. B., Massey, P. V., Molnar, E., Bashir, Z. I., and Cho, K. (2006) *Nat. Neurosci.* **9,** 170–172
63. Massey, P. V., and Bashir, Z. I. (2007) *Trends Neurosci.* **30,** 176–184
64. Bassell, G. J., and Warren, S. T. (2008) *Neuron* **60,** 201–214
65. Huber, K. M., Gallagher, S. M., Warren, S. T., and Bear, M. F. (2002) *Proc. Natl. Acad. Sci. U.S.A.* **99,** 7746–7750
66. Park, S., Park, J. M., Kim, S., Kim, J. A., Shepherd, J. D., Smith-Hicks, C. L., Chowdhury, S., Kaufmann, W., Kuhl, D., Ryazanov, A. G., Huganir, R. L., Linden, D. J., and Worley, P. F. (2008) *Neuron* **59,** 70–83
67. Berry-Kravis, E., Hessl, D., Coffey, S., Hervey, C., Schneider, A., Yuhas, J., Hutchison, J., Snape, M., Tranfaglia, M., Nguyen, D. V., and Hagerman, R. (2009) *J. Med. Genet.* **46,** 266–271
68. Hagerman, R. J., Berry-Kravis, E., Kaufmann, W. E., Ono, M. Y., Tartaglia, N., Lachiewicz, A., Kronk, R., Delahunty, C., Hessl, D., Visootsak, J., Picker, J., Gane, L., and Tranfaglia, M. (2009) *Pediatrics* **123,** 378–390
69. Kinney, G. G., O'Brien, J. A., Lemaire, W., Burno, M., Bickel, D. J., Clements, M. K., Chen, T. B., Wisnoski, D. D., Lindsley, C. W., Tiller, P. R., Smith, S., Jacobson, M. A., Sur, C., Duggan, M. E., Pettibone, D. J., Conn, P. J., and Williams, D. L., Jr. (2005) *J. Pharmacol. Exp. Ther.* **313,** 199–206
70. Uslaner, J. M., Parmentier-Batteur, S., Flick, R. B., Surles, N. O., Lam, J. S., McNaughton, C. H., Jacobson, M. A., and Hutson, P. H. (2009) *Neuropharmacology* **57,** 531–538